Internal Report
DESY F41
HASYLAB 81/06
June 1981

INVESTIGATION OF IONIC CRYSTALS WITH SYNCHROTRON RADIATION

by

G. Zimmerer

INVESTIGATION OF IONIC CRYSTALS WITH SYNCHROTRON RADIATION

G. Zimmerer

II. Institut für Experimentalphysik der Universität Hamburg,
Luruper Chaussee 149, 2000 Hamburg 50, West Germany

1. Introduction

Investigation of ionic crystals with synchrotron radiation (SR) illustrates very well the rapidly increasing importance of SR-excitation in, for example,

(i) conventional spectroscopy (like absorption, reflection)

(ii) modulation spectroscopy

(iii) photoelectron spectroscopy

(iv) luminescence and defect formation.

The main goal of (i) to (iii) is the investigation of the electronic structure. The fate of an elementary excitation manifests itself in (i) and (ii) only in line shapes. (iii) is an important link between an excitation and its decay products and thus also a link to (iv) which probes the long living excited states of a relaxed environment.

It is not possible to cover the whole range of experimental methods and physical problems indicated above in a short paper. It is indispensable to concentrate on a few topics. This seems to be legal, because systematic review articles[1-4] and even a data collection on alkali halides[5] exist. The few topics discussed in this paper shall demonstrate the potential power of experiments using SR-excitation. This is especially true for (iv). Though the field of SR-excited luminescence of ionic crystals is not well developed up to now, it will cover a substantial part of this paper in view of the general theme of this conference.

2. Some remarks on the use of SR in spectroscopy

The properties of SR were described elsewhere[1]. In short, we can summarize:

(i) SR has a continuous spectral distribution extending from the infrared to the x-ray region.

(ii) SR (of a storage ring) has a unique time structure. It consists of nearly δ-like light pulses (fwhm between ∿1 ns and .1 ns) with a high and precise repetition frequency (∿ 1 MHz to ∿ 500 MHz).

(iii) SR has a well defined polarization.

[+] to be published in the Proceedings of the Internat. Conference "Defects in Insulating Crystals" Riga, May 18-23, 1981 ed. by K.K. Shvarts.

(iv) SR is laser-like collimated.

Readers who are interested in more details including the various aspects of SR instrumentation are referred to references 1 and 6.

3. Optical Spectroscopy and Electronic Structure

3.1 General remarks

Conventional spectroscopic methods are used since long to investigate the onset of valence excitations of ionic crystals in the ultraviolet and near vacuum ultraviolet with conventional sources. The results could not be explained within simple bandstructure models. It turned out that excitonic effects play an essential and sometimes dominating role.

Spectroscopy of core excitations was scarce until SR became available. Core excitations are of special interest. Provided the band structure model is applicable, core spectra give direct information about the density of conduction band states, because core states are localized (core 'bands' are flat in $\vec{k}$ space). This expectation turned out to be by far too simple. In the following we shall concentrate on core excitations, because here the specific contributions of SR excitation are settled.

3.2 Alkali halides

The valence bands of alkali halides originate from the outermost p electrons of the anions. The conduction bands are predominantly cation s type at the bottom. With increasing atomic number of cations, d conduction bands come into play. The energetic positions of core excitations are given in Fig. 1. We start with the first cation core excitations (Na^+ 2p[7], K^+ 3p[8-14], Rb^+4p[12, 15-18] Cs^+ 5p[19,20]). As an example, in Fig. 2 high resolution reflectivity curves of in situ cleaved potassium halides are presented. A pronounced doublet (A_1, A_2) is found (nearly independent from the anion) and a pronounced maximum (C) which

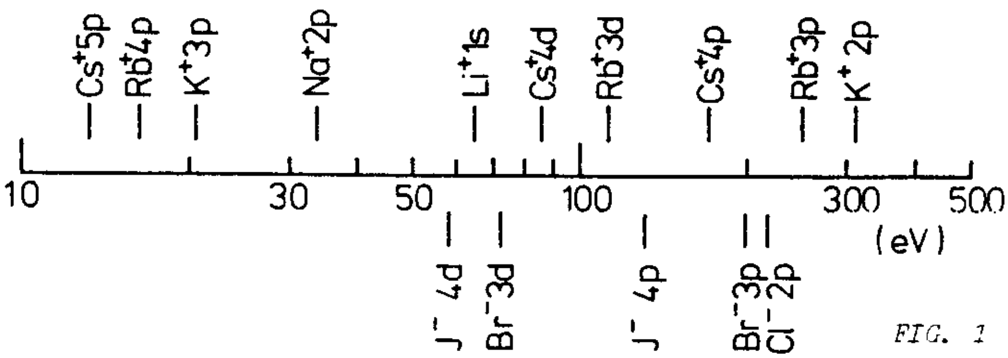

FIG. 1

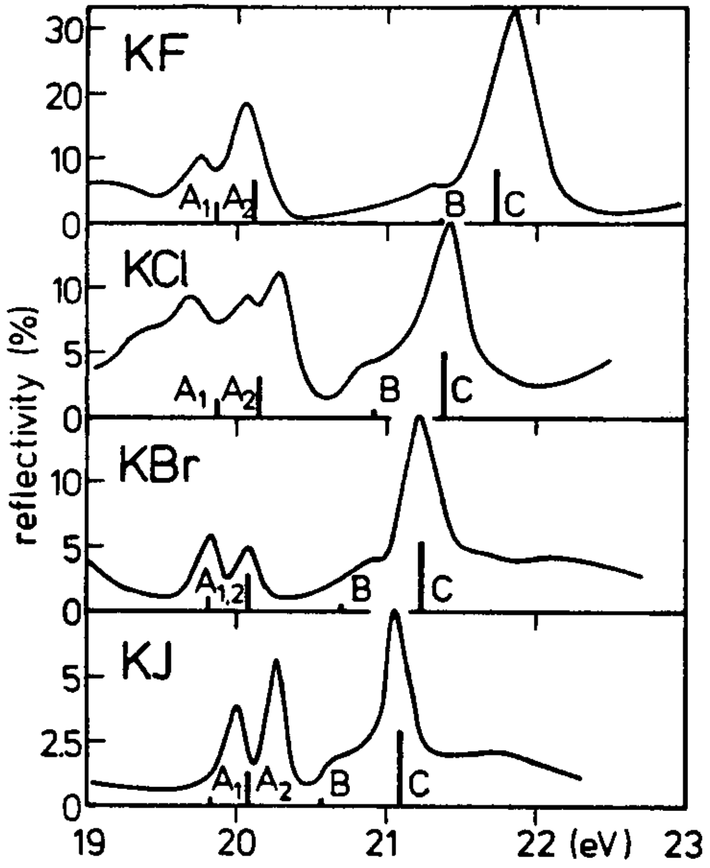

FIG. 2 Reflectivity of K halides at 22K (KF,KCl), 17K (KBr), 19K (KJ) in the region of K^+3p core excitons (Ref. 21).

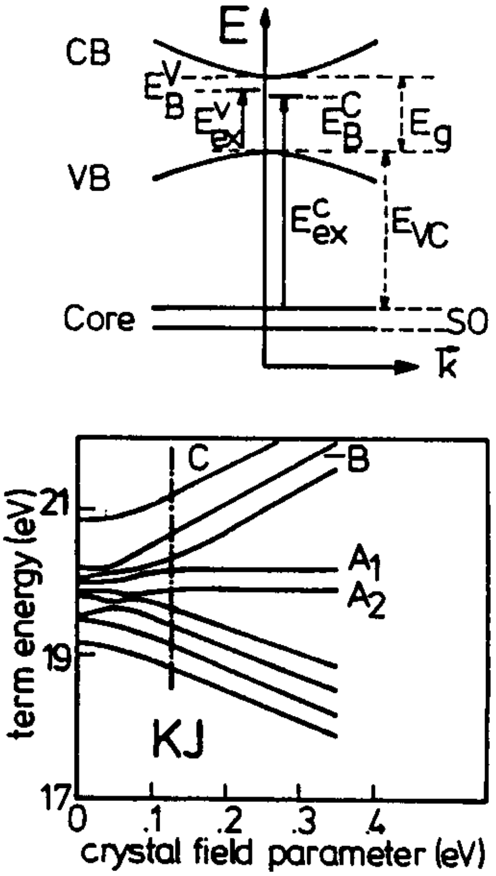

FIG. 3 Simplified illustration of band structure (Ref. 21) and ligand field model (Ref. 23).

shifts between 21 and 22 eV. Different models have been proposed for explanation (Fig. 3).

In the band structure model, the doublet is ascribed to core excitons in the center of the BZ. The splitting reflects the spin orbit splitting (SO) of the core hole (nearly identical with the free ion case). Peak C is explained as core exciton at point X of the BZ. The absence of a doublet structure (especially for K halides) is a result of exchange interaction[22].

The ligand field model starts from the multiplet split p^5 s and p^5 d configurations of the free ion which then is exposed to the crystal field[23]. The marks in Fig. 2 are the most intense transitions predicted by this model. Their heights are a measure for the calculated oscillator strength. With the technique of wavelength modulation, the sensitivity of the reflection curves was improved[18] and weaker structures predicted by the ligand field model could be detected.

A line shape analysis of K^+ 3p excitons disclosed a major contribution of exciton-phonon interaction[21]. Lattice relaxation energies and coupling constants were derived. In Ref. 12 the absorption features of KI above K^+3p excitons were compared with the density of states of the conduction band[24]. Good agreement was obtained (see Fig. 8). The agreement has been questioned[25], because it may be based on an incorrect value of binding energy E_B^C of the core excitons.

At higher energies, Cl^- 2p absorption spectra[24,26,27] were explained via density of states effects[24]. They show similarities to valence excitation (valence electrons are also p-type and fairly well localized at the anions). Excitonic effects are less important than in cation p-excitations, because the anion core is better screened by valence electrons than the cation core[25].

Of special interest are excitations of d-electrons (I^-4d[28], Rb^+3d and Cs^+4d[29]). From atomic physics it is known that d → f transitions are suppressed at threshold by a potential barrier, the oscillator strength being shifted to higher energies[30] (huge broad resonances). It turns out that the atomic nature of these transitions persists in the solid. Fig. 4 compares Cs^+4d absorption of molecular and crystalline CsCl[31]. At the onset of d → f transitions, faint lines due to d → p excitations are superimposed.

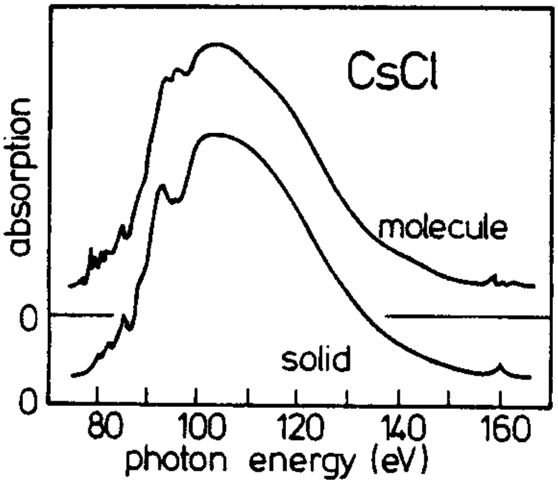

FIG. 4 Comparison between Cs^+4d absorption in molecular and solid CsCl (Ref. 31).

Li^+ 1s excitations are subject of controversial discussion (details see, e.g., in Ref. 32). They are parity forbidden at threshold. In absorption[33-35], faint and pronounced structures are found between ∿ 50 and 70 eV. The first thermomodulated transmission spectra in this energy range perhaps clarified the situation[36] (Fig. 5). The most prominent peak at 61.9 eV is ascribed to

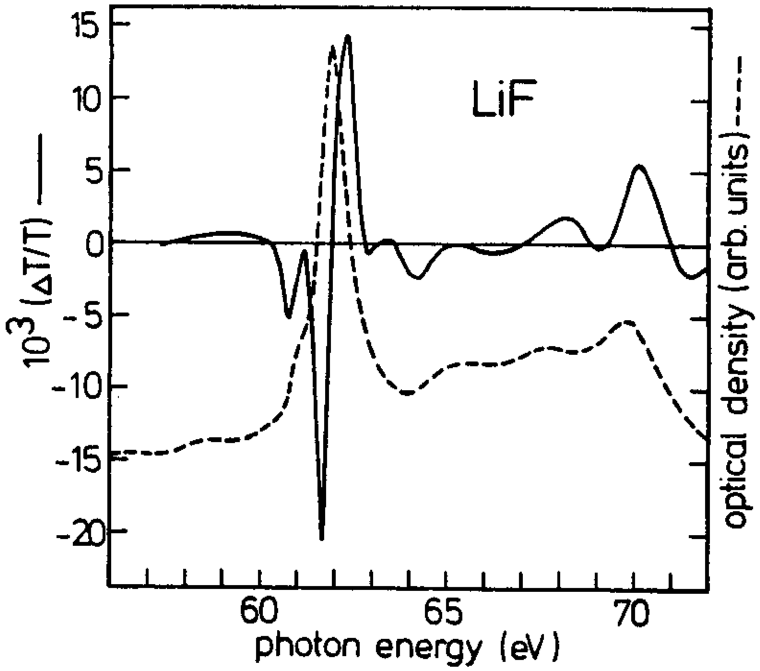

FIG. 5 Room temperature absorption and thermotransmission spectrum of a LiF film (230Å) on an Al substrate (630Å) (Ref. 36).

Li^+ $1s^2$ → 1s 2p transition[37] (exciton bound to a high conduction band with Li^+ 2p character[35]). Members of a forbidden exciton series at 60.8 and perhaps 62.1 eV bound to the s-type conduction band were established. They seem to have a moderate binding energy (∿ 1.7 eV). The binding energy of the allowed exciton seems to be exceedingly high (∿ 10 eV)[36].

Among the experiments on valence excitations the papers on reflection of the fluorides in the 6 to 35 eV region[38] and on thermoreflectance (LiF) between 10 and 30 eV[39] have to be mentioned. Due to the lack of space, discussion of solid solutions of alkali halides is also suppressed (Cl^- 2p excitation in KCl-NaCl[40], KCl-RbCl[41]; valence excitations in RbF-CsF[42]).

3.3 Alkaline earth halides

The outermost anion p electrons form the valence bands and cation s and d states the conduction bands. The first core excitations are cation p excitations as in alkali halides. Systematic reflectance investigations have been carried out for CaF_2, SrF_2, BaF_2[10, 13, 43] and $SrCl_2$[44] covering interband and Ca^{2+} 3p (∿ 24 eV), Sr^{2+} 4p (∿ 22 eV), Ba^{2+} 5p (∿ 16 eV) transitions. Mg halides[45] and Mg, Ca, Sr, Ba halides[46] were also investigated between 50 and 150 eV (absorption).

Valence excitations yield strong excitonic effects. The fluorides show also sharp and extremely strong cation p-core excitons which are sensitive to temperature[10, 13]. Cation p-core excitations at higher energies have broad pronounced structures. Comparison with alkali halides leads to the interesting conclusion that they are correlated with the coordination of cations in the lattice[10, 13]. This is explained by the local character of both the initial and the final states. In $SrCl_2$, localization is not so pronounced. Sr^{2+} 4p excitons are weaker than in SrF_2.

Mg^{2+} 2p core excitons yield considerable deviation from j-l coupling which manifests itself in relative intensities and the splitting of the doublets. The soft x-ray spectra of Mg halides up to 150 eV are similar to those of isoelectronic rare gases[45,46].

3.4 Rare earth halides

The electronic properties are determined by the localized rare earth 4f electrons and the band electrons of both ions. Reflectivity was measured with $\vec{E}\ ||$ and $\perp \vec{c}$ for La, Ce, Pr, NdF_3[47] and for La to GdF_3[48] between 10 and 35 eV, covering excitations of rare earth 5p core states and interband transitions. Surprisingly, the interband transitions yield no evidence for exitons. Rare earth 4f → 5d, 6s absorption spectra below 10 eV[48] are similar to those of rare earth ions doped into LaF_3[49]. They have broad maxima due to the delocalized nature of the final states in contrast to the sharp lines within the $4f^n$ configuration.

Interband absorption of La, Ce halides[50] was compared with Cl^- 2p spectra (overall profiles alike, deviations at threshold). The 4d absorption spectra[51] consist of sharp lines at the onset (100 to 115 eV) independent of the anion, and a broad continuum (120-130 eV). The sharp lines stem from $4d^{10}\ 4f^n \longrightarrow 4d^9\ 4f^{n+1}$ transitions. The broad continuum is due to transitions into f-symmetric continuum states.

3.5 Transition metal halides

The interesting aspects introduced by the d-bands of these materials can only be touched. Cl^- 2p absorption was investigated for MCl_2 (M = Mn, Fe, Co, Ni; Cu, Zn, Cd, Pb) and compared with Cl^- 3p interband transitions[52]. Similar measurements are reported for AgCl and TlCl[53] and AgCl, AgBr[54]. M^{2+} 3p absorption between 40 and 50 eV in MCl_2, MBr_2 (M = Cr, Mn, Fe, Co, Ni) was compared with the corresponding spectra of the metals. The energetic position of the d-bands could be deduced[55].

In perovskite type compounds KMF_3 (M = Mn, Fe, Co, Ni, Cu, Zn) (absorption up to 35 eV[56], reflection (M = Co, Ni, Mn, $RbMnF_3$)[57]) forbidden d → s transitions were established below the principal band edge with its strong excitons.

At higher energies, K^+ 3p core excitons show up. The ligand field model[23] seems to fail in these substances[56].

From recent reflection spectra (up to 30 eV) of Cu halides detailed band structure parameters were derived[58]. Some features are characterized through the whole sequence (CuCl → CuI) by their thermal behaviour and by their evolution with increasing spin orbit separation.

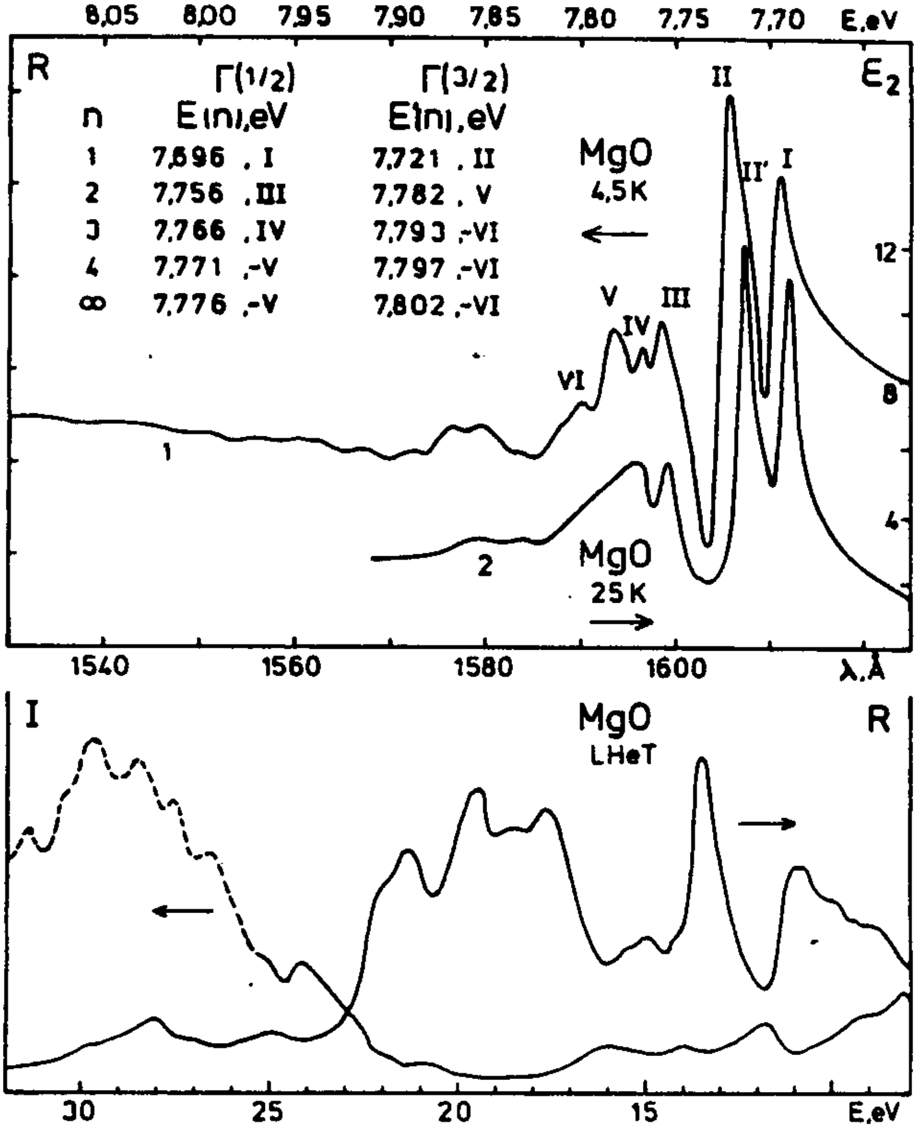

FIG. 6 Curve 1 (Ref. 61): Reflectivity of MgO crystals. Curve 2: ε_2 of MgO for comparison (Ref. 62). Lower part: reflectivity and luminescence excitation spectrum of MgO:Al (Ref. 61).

3.6 Ionic oxides

Optical investigations on oxides with SR are scarce so far. Reflection of BeO, ZnO, CdO and MgO single crystals was measured up to 30 eV[59] and of powder samples (MgO, CaO, SrO) up to 40 eV[60]. Recently, a detailed study was carried out on MgO single crystals[61] including reflection and luminescence excitation spectra. In Fig. 6, a reflection spectrum obtained at 4.5 K is shown and compared with earlier results[62] measured with a conventional source. The progress achieved with SR is obvious. Different members of two spin orbit split Wannier type exciton series can now be identified. The lower part of Fig. 6 contains a reflection curve at high photon energies which is in good agreement with Ref. 59 and a luminescence excitation spectrum (see sec. 5).

4. Photoemission Measurements

Because of the superior properties of the SR source, in photoemission very different problems are attacked like:

(i) position of energy levels relative to some reference
(ii) band structure parameters (density of states, dispersion of bands)
(iii) inelastic scattering of photoelectrons (thresholds, etc.)
(iv) nature and decay modes of core excitations
(v) matrix element effects
(vi) surface versus bulk states.

Especially the tunability of SR over a broad range of photon energies is of major importance for such experiments. The overwhelming number of experiments was carried out with alkali halides.

4.1 Yield measurements

In yield spectra, the total number of photoelectrons is measured as a function of excitation energy. A low resolution kinetic energy analysis is achieved with retarding grids. Yields have been measured on in situ evaporated films of alkali halides (∿ 50 to some thousand Å thickness). Typical examples are shown in Fig. 7[63]. The gross features are two structured maxima. The decrease around 2 E_g (E_g: band gap energy) marks the onset of inelastic electron electron scattering, the scattered electrons being unable to leave the crystal (scattered states below the vacuum level). More precisely, the scattering threshold is $E_g + E_x$ (E_x: exciton energy)[64, 65].

After a pronounced minimum the yield rises again and exceeds unity[65, 66], because the scattered electrons more and more reach final states above the vacuum level. Surprisingly, the K^+ 3p excitons show up as peaks, though they cannot escape directly. The peaks stem from decay products (see 4.2). Above $E_{vc} + 2\ E_g$ (E_{vc}: energy between core and top of valence band) the yield decreases again, because now electrons which stem from K^+ 3p continuum excitations are scattered below the vacuum level.

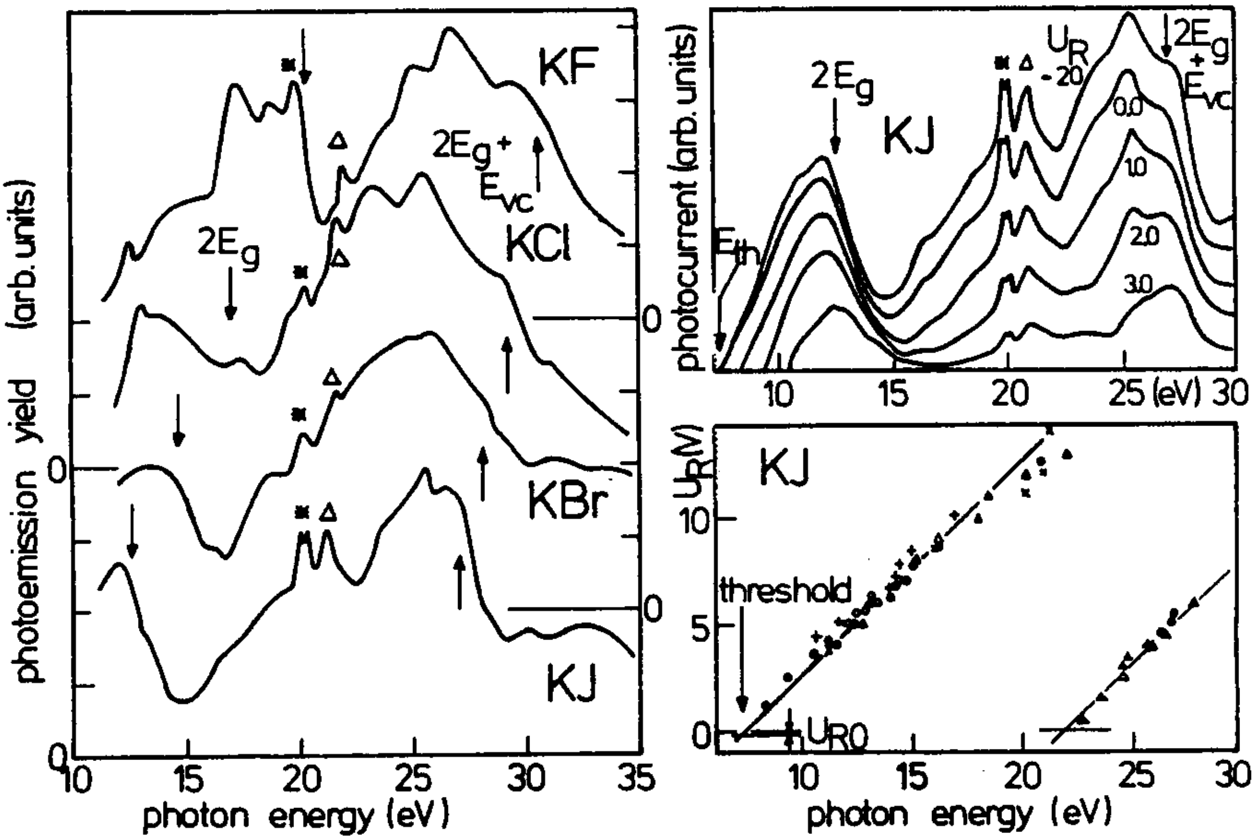

FIG. 7 Left part: photoelectric yield curves of K halides (normalized to the incident intensity). '+' marks the A doublet, 'Δ' the C-peak (Ref. 63). Right part: spectral distribution of photocurrent for different retarding potentials and plot of the stopping potential lines for valence band and K^+ 3p excitations in KJ (Ref. 67).

Fig. 7 also shows yields with retarding potentials and plots of stopping potentials of valence and core excitations[67]. Numerical values for photoemission threshold E_{th}, E_{vc}, electron affinity E_A and the binding energy E_B^C of K^+ 3p core excitons were extracted. E_B^C is comparable to the binding energy of valence excitons.

Besides the potassium halides[63,64,66,67], NaCl[68], RbCl[69] and Rb halides[65] were examined in a similar way. There exist also unpublished systematic yield measurements of Cs halides[70].

4.2 Decay products of core excitons

The first true alkali halide energy distribution curves (EDCs) enabled a detailed insight into the decay products of K^+3p excitons[71-73]. Auger decay and direct decay into the continuum of valence excitations compete with each other. They result in electrons in the conduction band with different kinetic energies. It was found that Auger decay is ca. twice as probable as direct recombination. Within an uncertainty of .4 eV, lattice relaxation effects subsequent to the creation of core excitons were excluded[71]. A complete insight into the decay of core excitons, however, needs the investigation of the radiative decay channel, even if the quantum efficiency may be small. The nature and decay products of Na^+2p core excitons in NaCl will be discussed in 4.4.

4.3 Band structure parameters

Below threshold of $e^- - e^-$ scattering, the mean free path of photoelectrons in alkali halides may exceed 100 Å. Moreover, the vacuum level roughly coincides with the bottom of the conduction band. Therefore, EDC's of scattered electrons ('secondaries') project the density of states of the conduction band, provided the scattering cross-section is only a smooth function of energy. From the secondaries, the conduction band density of states of KI has been extracted[72,73]. The experimental result is compared with theory[24] in Fig. 8. Moreover, the absorption curve mentioned in 3.2 is included[12]. Good agreement is found between the three curves.

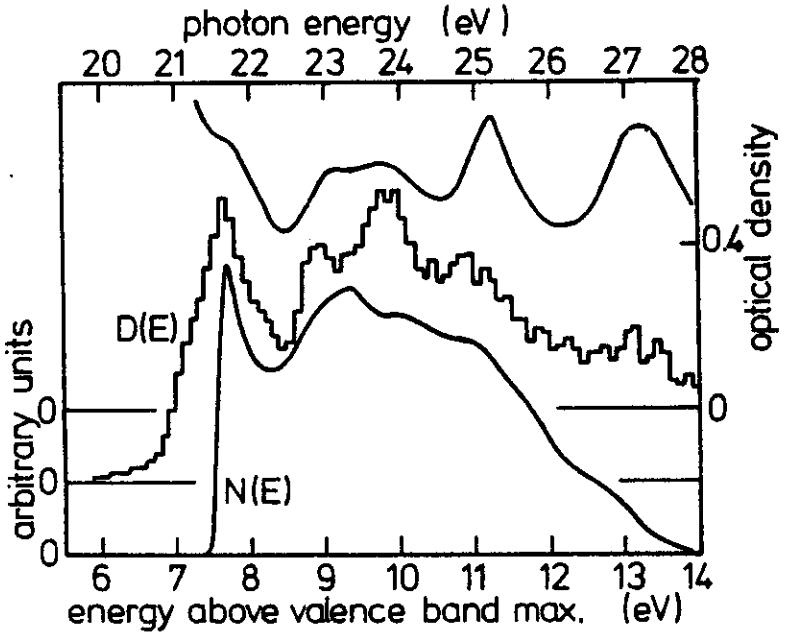

FIG. 8

Comparison between K^+ 3p continuum absorption (Ref. 12), calculated (Ref. 24) and measured (Ref. 72) density of conduction band states.

A break-through was achieved with angular resolved photoemission of alkali halide single crystals[74, 75]. The charging problem was overcome with a thermal source of electrons for compensation purposes. As an example, in Fig. 9 a polar diagram of photoemission intensity of KCl(100) surface is shown (polar angle θ = 45° fixed)[74]. An appropriate choice of excitation energy and kinetic energy of photoelectrons allows to discriminate between scattered and unscattered electrons and to measure the patterns for well defined initial and final states. The dispersion of valence and conduction bands of NaCl along the Γ-X direction could be deduced[75].

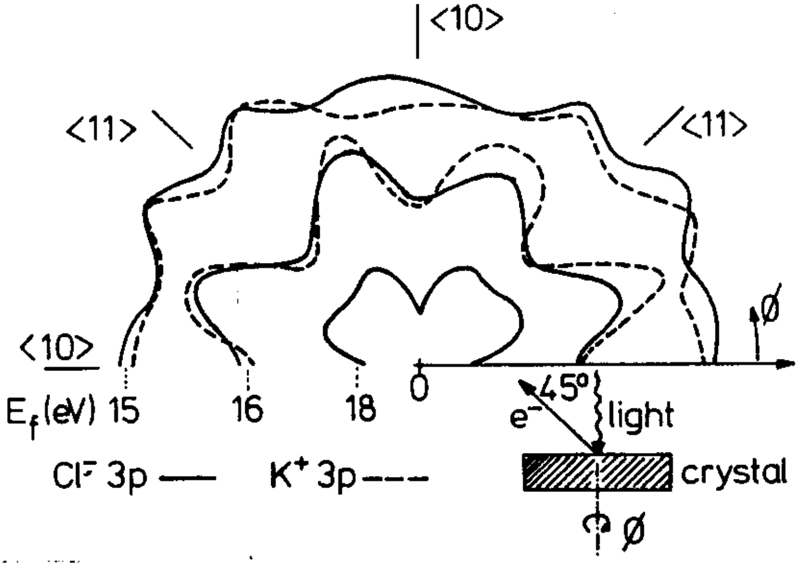

FIG. 9

Polar diagram of the photoemission intensity for the KCl(100) face at fixed polar angle (45°) for three final state energies and two initial state energies (Ref. 74).

4.3 Other problems

Positioning of core levels relative to the valence band is an interesting problem for the Li^+ 1s core state in LiF (see 3.2). From yield spectra and EDCs under excitation with 120 eV photons, $E_{VC} = 50.2$ eV was found[76]. Weak structures in the yield at ∿ 54 eV were interpreted as threshold of the parity forbidden 1s → 2s transitions, in accordance with Ref. 35, but in contrast to the results of thermotransmission measurements (3.2).

Photoelectron spectroscopy is also suited to investigate the line-widths of core states. In alkali halides they are considerably larger than Auger widths. From temperature dependence (Na^+ 2p, Cl^- 2p, Na^+ 2s) in NaCl, a large contribution of exciton phonon coupling was derived[77]. Similar to K^+ 3p excitons[21], the core excitations in NaCl can be described in a configuration coordinate diagram.

With the method of constant final state spectroscopy (CFS), in the case of Na^+ 2p excitation, both the decay of (lattice) relaxed and unrelaxed core excitons were observed. With this new information it was possible to discriminate between two groups of core excitons, namely Frenckel type excitons and autoionizing excitons[78].

Finally we have to mention that in NaCl, associated to Na^+ 2p, surface core excitons have been found[79]. This was only possible due to the tunability of the SR source. Surface sensitivity can be enhanced when an excitation energy is chosen at which the escape depth of unscattered electrons is extremely small.

4.4 Two-photon photoemission

Though this kind of experiment has not been applied to alkali halides up to now, it has to be mentioned, because it will open new possibilities in the near future. In the case of the isoelectronic rare gas solids recently a combination of SR excitation and laser excitation was used in photoemission[80, 81]. With the SR pulses (fwhm ca. .15 ns) valence excitons below the vacuum level were created (Kr). These excitons cannot lead to photoemission. However, time-correlated to the SR pulse, the excitons were ionized with a pulsed N_2 laser. The conduction electron produced in this way can be measured in photoemission. The energy distribution of such photoelectrons, for a fixed time delay between SR and laser pulse, may reveal direct information about the relaxation phenomena occurring in these materials.

5. Photoluminescence with SR-Excitation

5.1 General remarks

Photoluminescence experiments on ionic crystals with SR-excitation are still scarce. A typical set-up which includes the possibility of spectral and time analysis of luminescence under selective SR-excitation is described in Ref. 82.

In general, photoluminescence experiments clarify

(i) the physical nature of the radiating states

(ii) the formation of radiating centers

(iii) non-radiative relaxation processes.

SR is a well suited excitation source to attack all fields mentioned above due to the tunability over a broad spectral range combined with the unique time structure. However, systematic time and spectrally resolved investigations like in rare gas solids[83] have not been carried out so far.

5.2 Alkali halides

Predominantly Excitation spectra of either activator or intrinsic luminescence were measured over a wide range of photon energy. The spectral features give insight into the migration of elementary excitations, inelastic scattering processes and decay of core excitons. The first experiments were carried out on NaCl : Ag and KBr : Tl[84] and lateron extended to KCl : Tl, KCl : Cu, KCl : Pb[85]. The luminescence excitation spectra measured up to ∿ 40 eV are practically independent of the activators, but sensitively depend on the host. This is a direct proof that host excitation and host relaxation preceed popu-

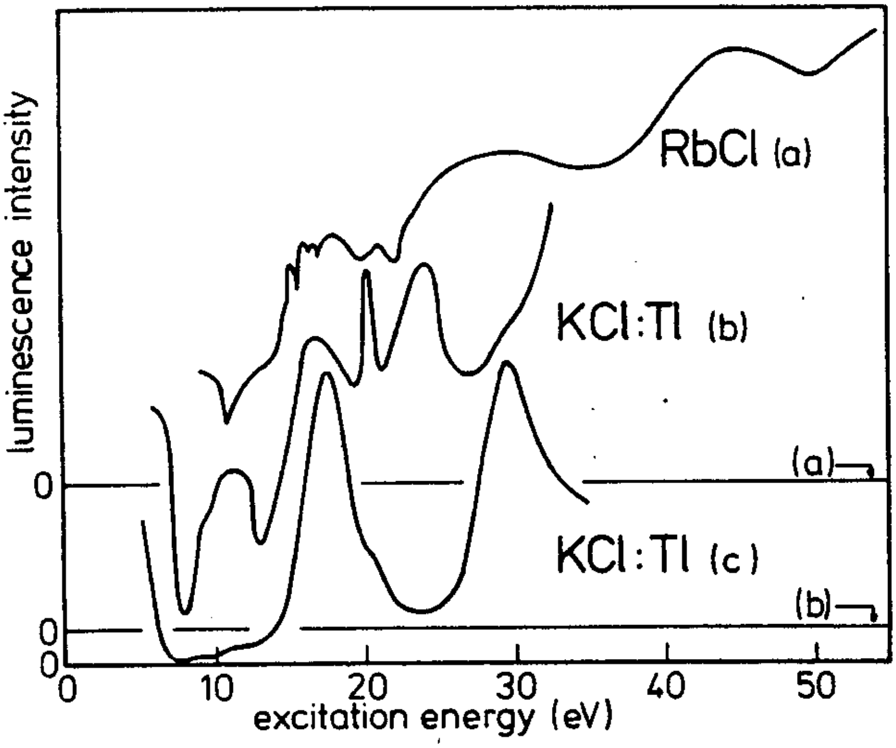

FIG. 10 Luminescence excitation spectra of KCl:Tl (c) (Ref. 84, 85), KCl:Tl (b) (Ref. 86) and RbCl (a) (Ref. 87).

lation of radiating states. In a first step, holes are trapped at the activator ions and then slowed down photoelectrons are captured leading to recombination luminescence. In Fig. 10, one of the results is included. Whereas in Refs. 84, 85 the overall behaviour of the excitation spectra is discussed in terms of electron-electron scattering and energy dependence of the recombination cross-section, lateron[86], clearly the effect of "photon multiplication" was identified in KCl : Tl and NaCl : Ag. This effect means that inelastic scattering leads to additional elementary excitations which can lead to photoluminescence themselves. So, all together, the quantum efficiency may exceed 1. In KCl:Tl a stepwise increase of luminescence intensity for excitation energies around 2 E_g and 3 E_g was found[86]. Discrimination between rapidly decaying luminescence and the slow recombination luminescence (measured 1 sec after excitation) is - in a certain sense - a first step to a partial cross-section excitation spectroscopy. In the rapid fraction of luminescence, bound electron-hole pairs (excitons) are the precursors of the activator luminescence, whereas in the slow process free electron hole pairs are the precursors of recombination luminescence[86].

From more detailed excitation spectra of the intrinsic luminescence of NaCl, NaBr, RbCl and RbBr[87] it was concluded that electron-electron scattering has a pronounced onset already at the energy $E_g + E_x$ (E_x: energy of $n = 1$ excitons). This leads to stepwise increases in the excitation spectra at energies $E_g + n \cdot E_x$, where n is an integer. For comparison purposes one typical curve is included in Fig. 10. The obvious differences between all three curves may be due to the fact that different luminescence channels have been monitored, but it may also be a consequence of different sample preparations, surface conditions, etc.

In the case of KI, both luminescence spectra under selective excitation and excitation spectra of spectrally selected luminescence bands have been studied[88]. The left part of Fig. 11 displays the self-trapped exciton luminescence of KI at 80 K with its π band at 3.34 eV and its σ band at 4.15 eV for various excitation energies. The right part (upper) curves show the excitation spectra of both bands. A remarkable difference between both spectra concerns the behaviour of $n = 1$ excitons (5,86 eV) which predominantly lead to the π, but not to the σ band. In the π band excitation spectrum one can identify a phonon

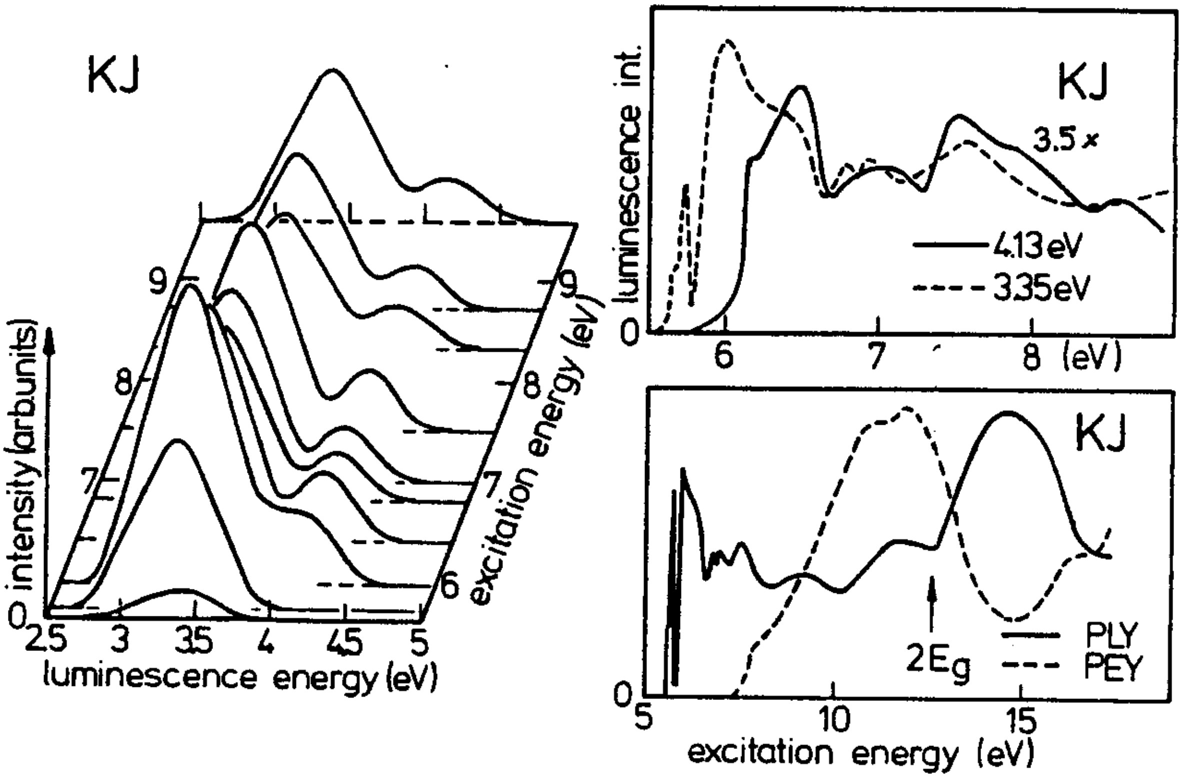

FIG. 11 Luminescence spectra of KJ for various excitation energies at 80 K. Excitation spectra of the spectrally selected luminescence bands (upper right part). Comparison of integral luminescence excitation spectrum (PLY, Ref. 88) and photoemission yield (PEY, Ref. 67).

sideband to the n = 1 exciton. The minima in the excitation spectra in the excitonic region, which correspond to absorption maxima, can be used to analyze the migration of excitons to the surface and surface quenching[89]. In the lower right part of Fig. 11 a comparison is made between the excitation spectrum of integral luminescence[88] and photoemission yield[67]. It shows that both yields have supplementary information concerning electron-electron scattering above $\sim 2\ E_g$.

In the early experiments discussed above, excitation intensity was too low for the observation of free exciton luminescence. A new experimental set-up will overcome this problem in the near future[90].

5.3 Alkaline earth compounds

Investigation of excitation spectra dominate. Room temperature results on thin evaporated films of CaS : Bi, SrS : Bi (10-40 eV) yield the "photon multiplication" effect like in alkali halides[60]. The x-ray part of SR was used to excite the very important, radiation damage resistant MgO and BeO single crystals[91]. Activator luminescence due to natural impurities like Al (5.4 eV in MgO) was observed together with strong emission bands at 6.8 eV in MgO and 6.7 eV in BeO, the nature of which could not be clarified.

The recent investigation of MgO already mentioned[61] includes measurement of the excitation spectrum of Al luminescence in MgO : Al (see Fig. 6, lower part). Surprisingly enough, the yield does not increase around $2\ E_g$ ($\sim$ 15.5 eV), but only above $\sim$22 eV. It is of comparable size between 7.6 and $\sim$ 22 eV. In this particular experiment, the length of excitation pulses is .15 ns. So, Al luminescence, which reaches its maximum only rather slowly, may not come into play in the usual way due to these ultrashort excitation pulses.

5.4 Rare earth compounds

Absorption and luminescence excitation spectroscopy were combined to study the excited states manifold of activator ions in $LaF_3 : Ce^{3+}$ and $LaF_3 : Pr^{3+}$ and the pumping mechanism of different luminescence lines and bands observed under state selective excitation. Especially, the energetic position and the Stark splitting of activator 5d bands were considered as well as pumping UV lasers via Pr^{3+} 5d and 6s bands[92, 93]. These investigations also include the first lifetime measurements on an ionic material using the unique time structure of SR[92]. The lifetime of the 5d → 4f luminescence of Ce^{3+} at 3050 Å in $LaF_3 : Ce^{3+}$ was determined (20 ns).

5.5 Other ionic luminescence materials

In ruby and MgO : Cr^{3+} the UV and VUV pumping mechanisms of the Cr^{3+} R-lines ($^2E_g \rightarrow {}^4A_{2g}$) were studied. Several charge transfer bands of the CrO_6^{3-} complex were established as pumping bands in the MgO and Al_2O_3 host. The R-line excitation spectra (3 - 30 eV) in ruby were measured with radiation polarized $\parallel$ and $\perp$ to the c-axis.

Y_2O_3 was mentioned in Ref. 91. The authors report on "above edge" luminescence at ∿ 7 and 24 eV (E_g ∿ 5.5 eV). Of more practical relevance are investigations of a number of crystallophosphors, in particular luminophores for x-ray screens. As an example we mention $Ba_3(PO_4)_2$: Eu[95]. This material has a constant energy output of luminescence between ∿ 20 eV and 2000 eV photon energy of excitation.

In α-Al_2O_3 the recombination luminescence yield is strongly increasing between ∿ 100 eV and 250 eV[96]. This is ascribed to the increasing penetration depth of exciting radiation. At lower energies, via ambipolar diffusion, the generated electron hole pairs have a chance to reach the surface (surface quenching).

Finally, we mention investigations which concentrate on the problem of pumping solid state lasers with the x-ray part of SR[97, 98]. Among others, as a promising example, NaCl : J is discussed. This field needs additional work.

6. Defect Formation in Ionic Crystals

Already in 1970, the coloration of KCl and KBr crystals with photons of an energy between 40 and 150 eV was investigated[99]. A combination of metal film filters enabled to measure the energy dependence of coloration. The visible part of SR was used to monitor F-center production. Fig. 12 shows the number of F-centers per cm^2 as a function of absorbed energy. The energy required to produce one F-center decreases with increasing photon energy and is considerably higher than under uniform volume irradiation. This effect is explained by surface sensitivity. The ultimate concentration of F centers produced in this way was ∿ $10^{19} cm^{-3}$.

More recently, SR has been spectrally dispersed and then used to produce radiation damage in a variety of inorganic and organic materials including some ionic crystals at low temperature (LNT) (50-400 Å)[100]. An E.S.R. spectrometer was used to look for evidence of radiation damage. The rate at which radiation damage was produced proved to be slower than originally expected, but on the other hand the work has shown the feasibility of using monochroma-

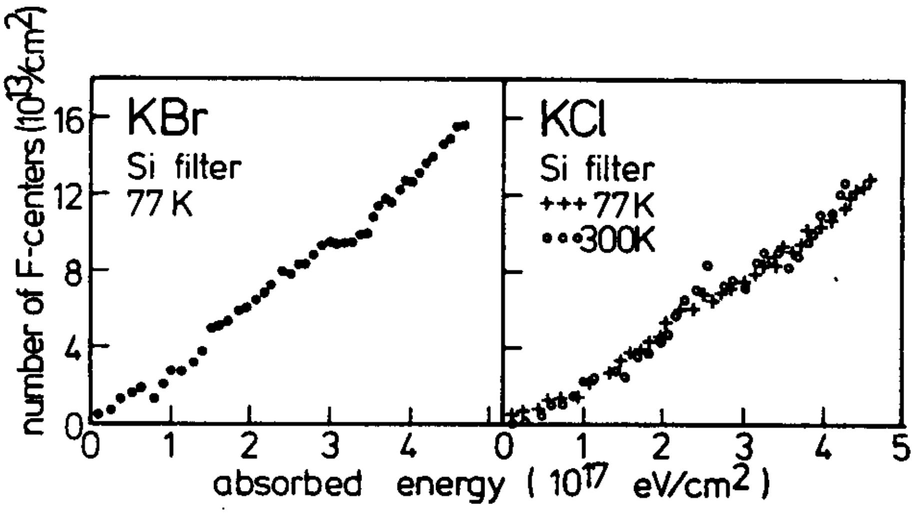

FIG. 12

Coloration of KBr and KCl (Ref. 99).

tized SR in this area of research.

Finally, an investigation concerning the existence of core excitons at the Cl^- 2p edge in NaCl : Ag has to be mentioned[101]. The samples were irradiated with photons of various energies. After each irradiation, thermoluminescence was recorded. The integrated thermoluminescence intensity, which is normalized to the number of absorbed photons, represents the efficiency of carrier storage in NaCl : Ag at Ag^+ centers created by the exciting photons. In this way, an "electron + two valence holes" complex as a result of Auger decay of Cl^- 2p excitons was established.

7. Summary

SR experiments contributed significantly to a better understanding of the electronic structure of ionic crystals. This will be true also in the future. However, more and more experiments will deal with secondary effects, especially with luminescence and defect formation. Even SR photoemission will be of great importance to investigate decay products and relaxation phenomena. The unique time structure of SR will be used for time resolved spectroscopy down to the sub-ns region as it has already been done with rare gas solids[83].

Acknowledgement

I would like to thank Dr. I. Kuusmann from Tartu, Estonian SSR, for many helpful discussions and a critical reading of the manuscript during his stay at DESY-HASYLAB.

References

1. see, e.g., *Synchrotron Radiation* (Topics in Current Physics vol. 10), ed. by C. Kunz, Springer Verlag, Heidelberg 1979
2. Collection: *Physics of Vacuum Ultraviolet Radiation* (in Russian), Naukova Dumka Press, Kiev 1974
3. R. Haensel, in *Festkörperprobleme vol. 15* (Vieweg, Braunschweig 1975), p. 203
4. E.E. Koch, C. Kunz and B. Sonntag, Phys. Reports 28C, 154 (1977)
5. R.P. Haelbich, M. Iwan and E.E. Koch, Physics Data 8-1 (1977) published by Zentralstelle für Atomkernenergie-Dokumentation (ZAED), 7514 Eggenstein-Leopoldshafen (Germany)
6. Proc. Intern. Conf. on Synchrotron Radiation Instrumentation, Orsay 1977, ed. F. Wuilleumier and Y. Farge, reprinted from Nuclear Instr. and Methods 152 (1978)
7. R. Haensel, C. Kunz, T. Sasaki and B. Sonntag, Phys. Rev. Letters 20, 1436 (1968)
8. D. Blechschmidt, R. Klucker and M. Skibowski, phys. stat. sol. 36, 625 (1969)
9. H. Saito, M. Watanabe, A. Ejiri, S. Sato, H. Yamashita, T. Shibaguchi, H. Nishida and S. Yamaguchi, Solid State Communic. 8, 1861 (1970)
10. G.W. Rubloff, J. Freeouf, H. Fritzsche and K. Murase, Phys. Rev. Letters 26, 1317 (1971)
11. D. Blechschmidt, R. Haensel, E.E. Koch, U. Nielsen and M. Skibowski, phys. stat. sol. (b) 44, 787 (1971)
12. H. Saito, Science of Light 20, 1 (1971)
13. G.W. Rubloff, Phys. Rev. B 5, 662 (1972)
14. F.A. Korolev and O.F. Kulikov, Opt. Spectrosc. 31, 442 (1971)
15. M. Watanabe, A. Ejiri, H. Yamashita, H. Saito, S. Sato, T. Shibaguchi and H. Nishida, J. Phys. Soc. Japan 31, 1085 (1971)
16. C.J. Peimann and M. Skibowski, phys. stat. sol.(b) 46, 655 (1971)
17. V. Saile, N. Schwentner, M. Skibowski, W. Steinmann and W. Zierau, Phys. Letters 46A, 245 (1973)
18. W. Zierau and M. Skibowski, J. Phys. C 8, 1671 (1975)
19. D. Blechschmidt, V. Saile, M. Skibowski and W. Steinmann, Phys. Letters 35A, 221 (1971)
20. V. Saile and M. Skibowski, phys. stat. sol. (b) 50, 661 (1972)
21. M. Skibowski, G. Sprüssel and V. Saile, Appl. Optics 19, 3978 (1980); G. Sprüssel, M. Skibowski and V. Saile, Solid State Communic. 32, 1091 (1979)
22. Y. Onodera and Y. Toyozawa, J. Phys. Soc. Japan 22, 833 (1967)
23. S. Satoko and S. Sugano, J. Phys. Soc. Japan 34, 701 (1973) In this paper, a detailed comparison between theory and experiment is given for Rb-halides 15.
24. F.C. Brown, Ch. Gähwiller, H. Fujita, A.B. Kunz, W. Scheifley and N. Carrera, Phys. Rev. B 2, 2126 (1970)
25. S.T. Pantelides, Phys. Rev. B 11, 2391 (1975)
26. T. Sagawa, Y. Igushi, M. Sasanuma, T. Nasu, S. Yamaguchi, S. Fujiwara, M. Nakamura, A. Ejiri, T. Masuoka, T. Sasaki and T. Oshio, J. Phys. Soc. Japan 21, 2587 (1966)
27. Y. Iguchi, T. Sagawa, S. Sato, M. Watanabe, H. Yamashita, A. Ejiri, M. Sasanuma, S. Nakai, M. Nakamura, S. Yamaguchi, Y. Nakai and T. Oshio, Solid State Communic. 6, 575 (1968)
28. H. Fujita, Ch. Gähwiller and F.C. Brown, Phys. Rev. Letters 22, 1369 (1969)

29. M. Cardona, R. Haensel, D.W. Lynch and B. Sonntag, Phys. Rev. B 2, 1117 (1970)
30. U. Fano and J.W. Cooper, Rev. Mod. Phys. 40, 441 (1968)
31. K. Radler and B. Sonntag, Chem. Phys. Letters 39, 311 (1976)
32. D. Lynch, in Ref. 1., p. 357
33. R. Haensel, C. Kunz and B. Sonntag, Phys. Rev. Letters 20, 262 (1968)
34. F.C. Brown, Ch. Gähwiller, A.B. Kunz and N.O. Lipari, Phys. Rev. Letters 25, 927 (1970)
35. B.F. Sonntag, Phys. Rev. B 9, 3601 (1974)
36. C.G. Olson and D.W. Lynch, Solid State Communic. 31, 51 (1979)
37. S.T. Pantelides and F.C. Brown, Phys. Rev. Letters 33, 298 (1974)
38. K. Kameswara Rao, T.J. Moravec, J.C. Rife and R.N. Dexter, Phys. Rev. B 12, 5937 (1975)
39. M. Piacentini, C.G. Olson and D.W. Lynch, Phys. Rev. Letters 35, 1658 (1975); M. Piacentini, Il Nuovo Cimento 39B, 682 (1977)
40. Y. Nakamura, M. Watanabe, S. Sato and Y. Nakai, Solid State Communic. 9, 2017 (1971)
41. M. Watanabe, J. Phys. Soc. Japan 34, 755 (1973)
42. M. Watanabe and K. Nishioka, J. Phys. Soc. Japan 45, 1670 (1978)
43. W. Hayes, E.E. Koch and A.B. Kunz, J. Phys. C 4, L 200 (1971)
44. A.J. Bourdillon and J.H. Beaumont, J. Phys. C 9, L 473 (1976)
45. P. Rabe, B. Sonntag, T. Sagawa and R. Haensel, phys. stat. sol. (b) 50, 559 (1972)
46. P. Rabe, thesis, University of Hamburg; Internal Report DESY F41-74/2, DESY, Hamburg
47. D.W. Lynch and C. Olson, Solid State Communic. 12, 661 (1973)
48. C.G. Olson, M. Piacentini and D.W. Lynch, Phys. Rev. B 18, 5740 (1978)
49. Wm. S. Heaps, L.R. Elias and W.M. Yen, Phys. Rev. B 13, 94 (1976)
50. S. Sato, J. Phys. Soc. Japan 41, 913 (1976)
51. S. Suzuki, T. Ishii and T. Sagawa, J. Phys. Soc. Japan 38, 156 (1975)
52. S. Sato, T. Ishii, I. Nagakura, O. Aita, S. Nakai, M. Yokota, K. Ichikawa, G. Matsuoka, S. Kono and T. Sagawa, J. Phys. Soc. Japan 30, 459 (1971)
53. S. Sato, M. Watanabe, Y. Iguchi, S. Nakai, Y. Nakamura and T. Sagawa, J. Phys. Soc. Japan 33, 1638 (1972)
54. N.J. Carrera and F.C. Brown, Phys. Rev. B 4, 3651 (1971)
55. S. Nakai, H. Nakamori, A. Tomita, K. Tsutsumi, H. Nakamura and S. Sugiura, Phys. Rev. B 9, 1870 (1974)
56. H. Onuki, F. Sugawara, Y. Nishihara, M. Hirano, Y. Samaguchi, A. Ejiri, H. Takahashi and H. Abe, Solid State Communic. 20, 35 (1976)
57. J.H. Beaumont, A.J. Bourdillon and J. Bordas, J. Phys. C 10, 333 (1977)
58. J.G. Gross, S. Lewonczuk, M.A. Khan and J. Ringeisen, Solid State Communic. 30, 181 (1979);
59. J.L. Freeouf, Phys. Rev. B 7, 3810 (1973)
60. V. Mikhailin, E.E.Koch and M. Skibowski, in *Vacuum Ultraviolet Radiation Physics*, ed. by E.E. Koch, R. Haensel and C. Kunz, Pergamon-Vieweg (Braunschweig 1974), p. 401
61. W. Böhmer, I. Kuusmann and G. Zimmerer, Annual Report 1980 of DESY-HASYLAB, Hamburg, p. 67; Verhandl. DPG (VI) 16, 232 (1981); this conference, collection of abstracts, p.427 ; I. Kuusmann, E. Feldbach and G. Zimmerer, Proc. Internat. Conf. on Luminescence, Berlin, July 1981, to be published in J. Luminescence
62. R.C. Whited and W.C. Walker, Phys. Rev. Letters 22, 1428 (1969)

63. D. Blechschmidt, M. Skibowski and W. Steinmann, Opt. Communic. 1, 275 (1970)
64. T. Sasaki, Y. Iguchi, H. Sugawara, S. Sato, T. Nasu, A. Ejiri, S. Onari, K. Kojima and T. Oya, J. Phys. Soc. Japan 30, 580 (1971)
65. Authors like in Ref. 64., J. Phys. Soc. Japan 30, 581 (1971)
66. H. Sugawara, T. Sasaki, Y. Iguchi, S. Sato, T. Nasu, A. Ejiri, S. Onari, K. Kojima and T. Oya, Opt. Communic. 2, 333 (1970)
67. D. Blechschmidt, M. Skibowski and W. Steinmann, phys. stat. sol. 42, 61 (1970)
68. R. Haensel, G. Keitel, G. Peters, P. Schreiber, B. Sonntag and C. Kunz, Phys. Rev. Letters 23, 530 (1969)
69. Y. Iguchi, T. Sasaki, H. Sugawara, S. Sato, T. Nasu, A. Ejiri, S. Onari, K. Kojima and T. Oya, Phys. Rev. Letters 26, 82 (1971)
70. V. Saile, Diploma work, University of Hamburg 1973; Internal Report DESY F41-73/12, DESY, Hamburg (1973)
71. G.J. Lapeyre, A.D. Baer, J. Hermanson, J. Anderson, J.A. Knapp and P.L. Gobby, Solid State Communic. 15, 1601 (1974)
72. A.D. Baer and G.J. Lapeyre, Phys. Rev. Letters 31, 304 (1973)
73. G.J. Lapeyre, J. Anderson, P.L. Gobby and J.A. Knapp, Phys. Rev. Letters 33, 1290 (1974)
74. F.J. Himpsel and W. Steinmann, Phys. Rev. Letters 35, 1025 (1975)
75. F.J. Himpsel and W. Steinmann, Phys. Rev. B 17, 2537 (1978)
76. W. Gudat, C. Kunz and H. Petersen, Phys. Rev. Letters 32, 1370 (1974)
77. M. Iwan and C. Kunz, Phys. Letters 60A, 345 (1977)
78. M. Iwan and C. Kunz, J. Phys. C 11, 905 (1978)
79. U. Rehder, W. Gudat, R.G. Hayes and C. Kunz, Proc. 7th Intern. Vac. Congr. & 3rd Intern. Conf. Solid Surfaces (Vienna 1977)
80. V. Saile, D. Rieger, W. Steinmann and T. Wegehaupt, Phys. Letters A 79, 221 (1980)
81. V. Saile, Applied Optics 19, 4115 (1980)
82. U. Hahn, N. Schwentner and G. Zimmerer, Nuclear Instr. and Methods 152, 261 (1978)
83. N. Schwentner, Applied Optics 19, 4104 (1980)
84. R. Onaka and H. Onuki, Extended Abstracts of the 3rd Intern. Conf. on VUV radiation physics Tokyo 1971, 30 p. A1-6
85. H. Onuki and R. Onaka, J. Phys. Soc. Japan 34, 720 (1973)
86. S.N. Ivanov, E.R. Il'mas, Ch.B. Lushchik and V.V. Mikhailin, Fiz. Tverd. Tela 15, 1574 (1973) / Sov. Phys. Solid State 15, 1053(1973)
87. J.H. Beaumont, A.J. Bourdillon and M.N. Kabler, J. Phys. C 9, 2961 (1976)
88. U. Hahn, Diploma work, University of Hamburg 1974, U. Hahn, R. Brodmann and G. Zimmerer, Verhandl. DPG (VI) 10, 419 (1975) and unpublished results
89. Ch. Ackermann, R. Brodmann, U. Hahn, A. Suzuki and G. Zimmerer, phys. stat. sol. (b) 74, 579 (1976)
90. P. Gürtler, E. Roick and G. Zimmerer, Annual Report of DESY-HASYLAB 1980 Hamburg, p. 52; P. Gürtler, M. Pouey and G. Zimmerer, Extended Abstracts of VIth Internat. Conf. on VUV Rad. Phys., Charlottesville 1980, III-25; H. Wilke, W. Böhmer and N. Schwentner, loc. cit., III-47
91. S.N. Ivanov, G.N. Kulipanov, I.N. Luchnik, V.V. Mikhailin, V.B. Khlestov and A.V. Khudyakov, Izv. Akad. Nauk SSSR Sev. Fiz. 41, N$^{\underline{o}}$ 7, 1326 (1977) / Bull. Acad. Sci. USSR 41, N$^{\underline{o}}$ 7, 10 (1977)
92. W.S. Heaps, D.S. Hamilton and W.M. Yen, Optics Communic. 9, 304 (1973)

93. L.R. Elias, W.S. Heaps and W.M. Yen, Phys. Rev. B 8, 4989 (1973)
94. W.M. Yen, L.R. Elias and D.L. Huber, Phys. Rev. Letters 24, 1011 (1970)
95. A.A. Sokolov, I.M. Ternov and V.V. Mikhailin, Izv. VUZ Fiz. (USSR) 19,7 (1976) / Sov. J. Physics 19, 403 (1976)
96. A.P. Zhurakovskii, E.S. Gluskin and M.A. Elango, Fiz. Tverd. Tela (Leningrad) 21, 233 (1979) / Sov. Phys. Solid State 21, 138 (1979)
97. V.V. Mikhailin, S.P. Chernov and A.V. Shepelev, Dokl. Akad. Nauk SSSR 237, 555 (1977) / Sov. Phys. Dokl. 22, 661 (1977)
98. R.V. Khokhlov, S.P. Chernov, P.B. Esselbakh, P.M. Lozovsky, I.N. Luchnik, V.V. Mikhailin and A.V. Shepelev, Nucl. Instr. and Methods 152, 265 (1978)
99. M. Elango, Ch. Gähwiller and F.C. Brown, Solid State Communic. 8, 893 (1970)
100. R.J. Booth, M.C.R. Symons and K.R, Lea, Radiat. Phys. Chem. 10, 315 (1977)
101. A.P. Zhurakovskii, E.S. Gluskin and M.A. Elango, Fiz. Tverd. Tela (Leningrad) 20, 1097 (1978) / Sov. Phys. Solid State 20, 633 (1978)